

# A Pseudomorphic AlGaAs/ $n^+$ -InGaAs Metal-Insulator-Doped Channel FET for Broad-Band, Large- Signal Applications

David R. Greenberg, *Student Member, IEEE*, Jesús A. del Alamo, *Member, IEEE*, James P. Harbison,  
and Leigh T. Florez

**Abstract**—We demonstrate MBE-grown  $L_g = 1.7\text{-}\mu\text{m}$  pseudomorphic  $\text{Al}_{0.38}\text{Ga}_{0.62}\text{As}/n^+\text{-In}_{0.15}\text{Ga}_{0.85}\text{As}/\text{GaAs}$  metal-insulator-doped channel FET's (MIDFET's) displaying extremely broad plateaus in both  $f_T$  and  $f_{\max}$  versus  $V_{GS}$ , with  $f_T$  sustaining 90% of its peak over a gate swing of 2.6 V. Drain current is highly linear with  $V_{GS}$  over this swing, reaching 514 mA/mm. We find no frequency dispersion in  $g_m$  up to 3 GHz, indicating the absence of electrically active traps in the undoped AlGaAs pseudoinsulator layer. These properties combine to make the pseudomorphic MIDFET highly suited to linear, large-signal, broad-band applications.

RECENT experiments on GaAs-based heterostructures have demonstrated that the metal-insulator-doped channel FET (MIDFET) can match many key figures of merit of the modulation-doped FET (MODFET) while avoiding several of its inherent drawbacks [1]. In particular, by removing all donors from the gate pseudoinsulator and placing them in the heavily doped channel layer, the MIDFET achieves a very large breakdown voltage  $V_B$  and a high transconductance  $g_m$  over an extremely broad gate-source voltage  $V_{GS}$  swing [2], [3], free from collapse due to pseudoinsulator donor-state filling [4]. As a result of the  $g_m$  plateau and extended forward gate bias, the MIDFET realizes high linearity in drain current  $I_D$  versus  $V_{GS}$  and very large values of both  $I_D$  and channel electron sheet density  $n_s$  [2], [3]. These features are further enhanced by using a pseudomorphic InGaAs channel to improve channel electron confinement [5], [6], and combine to make pseudomorphic MIDFET's well suited for a very important class of linear and high-power telecommunications applications including efficient microwave power amplifiers [7] and laser-diode drivers.

In this study, we experimentally demonstrate the pseudo-

morphic AlGaAs/ $n^+$ -InGaAs MIDFET's unique suitability for large-signal, broad-band operation, an area in which the MODFET exhibits severe limitations. We have fabricated devices with extremely broad plateaus in the  $V_{GS}$  dependence of  $g_m$ ,  $f_T$ , and  $f_{\max}$ , directly attributable to electron velocity saturation in the channel maintained over most of the useful gate swing. These plateaus are in contrast with the highly peaked characteristics of the MODFET [8], [9] and permit both accurate reproduction of large-signal, high-frequency transients as well as flexible circuit biasing. In addition, our devices show an almost complete lack of frequency dispersion in  $g_m$ , permitting extremely broad-band operation and indicating the absence of electrically active, deep-level traps in the undoped AlGaAs pseudoinsulator layer. Such dispersion is intrinsic to MODFET's [10] and has also been observed in MIDFET's reported to date [11].

The MBE-grown heterostructure, shown in Fig. 1, consists, from top to bottom, of a 50-Å GaAs cap, a 300-Å  $\text{Al}_{0.38}\text{Ga}_{0.62}\text{As}$  gate pseudoinsulator, a 150-Å  $n^+$ - $\text{In}_{0.15}\text{Ga}_{0.85}\text{As}$  channel ( $N_d = 4 \times 10^{18} \text{ cm}^{-3}$ ), a 100-Å GaAs electron confinement layer, a 1000-Å  $\text{Al}_{0.38}\text{Ga}_{0.62}\text{As}$  buffer/confinement layer, and a 1000-Å GaAs buffer, grown on a semi-insulating (100) GaAs substrate. Growth takes place under typical As-stabilized overpressure conditions using an As cracker, with an initial substrate temperature of 580°C maintained through the completion of the AlGaAs buffer. The substrate temperature is then ramped down during growth of the GaAs back confinement layer, reaching 530°C by the start of the InGaAs channel. A reduced temperature is necessary in order to avoid In reevaporation during channel growth and thus to obtain accurate temperature-insensitive InAs mole fraction control in that layer. This relatively low temperature is maintained for the remainder of the growth. Although previous studies have indicated that high-quality AlGaAs growth requires temperatures above 600°C [12], [13], we are able to obtain excellent AlGaAs crystal quality here at 530°C, possibly due to our use of a pre-cracked As source or to a low concentration of chamber impurities. High-purity growth in our Varian GEN II MBE growth system has been previously demonstrated. We have achieved two-dimensional electron gas mobilities of over  $1 \times 10^6 \text{ cm}^2/\text{V} \cdot \text{s}$  at 4.2 K in structures with a relatively

Manuscript received December 28, 1990; revised May 31, 1991. This work was supported by C. S. Draper Laboratory under Grant DL-H-404180 and by equipment grants from Bellcore and Hewlett Packard. D. R. Greenberg was supported by a Hertz Foundation Fellowship.

D. R. Greenberg and J. A. del Alamo are with the Department of Electrical Engineering and Computer Science, Massachusetts Institute of Technology, Cambridge, MA 02139.

J. P. Harbison and L. T. Florez are with Bell Communications Research, Red Bank, NJ 07701.

IEEE Log Number 9102191.

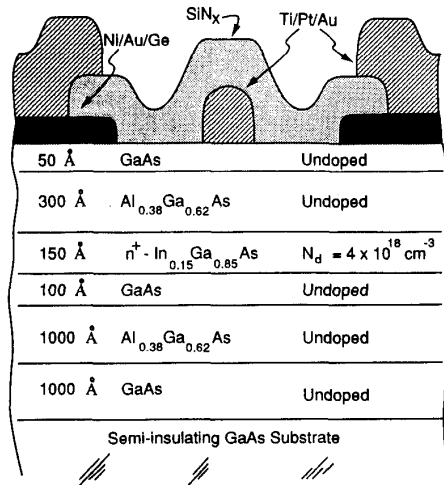


Fig. 1. Schematic cross section of the pseudomorphic  $\text{Al}_{0.38}\text{Ga}_{0.62}\text{As}/\text{n}^+\text{-In}_{0.15}\text{Ga}_{0.85}\text{As}/\text{GaAs}$  MIFET.

small 200-Å spacer as well as record low threshold currents of 0.35 mA in patterned quantum-well lasers [14].

Low-frequency and T-gate microwave MIFET's as well as diodes and a variety of test structures are fabricated using a non-self-aligned five-mask process with double-level metal and dielectric passivation. After a mesa etch for device isolation, we evaporate and pattern Ni/Au/Ge ohmic contacts and alloy them by RTA at 420°C for 10 s. We then form a Ti/Pt/Au gate-interconnect layer, followed by LPCVD deposition of 1750 Å of  $\text{SiN}_x$  at 190°C for passivation and intermetal isolation. Next, we etch via holes and pad openings in the dielectric using HF, and conclude fabrication with a final Ti/Pt/Au pad/interconnect layer. Our process provides high yields, permitting fabrication of working circuits as complex as a 13-stage ring oscillator. As a result, we report all data as statistical averages over many devices, unless otherwise stated.

Fig. 2 shows  $g_m$  and  $I_D$  versus  $V_{GS}$  for  $L_g = 1.7\text{-}\mu\text{m}$  and  $W_g = 30\text{-}\mu\text{m}$  MIFET's at  $V_{DS} = 3.5\text{ V}$ , obtained through a pointwise computer averaging of 20 randomly selected devices. We observe a peak  $g_m$  of  $165 \pm 5\text{ mS/mm}$ , with  $g_m$  maintaining over 90% of this value over a broad gate swing of  $1.65 \pm 0.11\text{ V}$  (tolerances are one standard deviation). By injecting current from gate to source with floating drain and measuring  $V_{DS}$ , we extract  $R_s = 1.53 \pm 0.10\ \Omega \cdot \text{mm}$ , yielding an intrinsic  $g_{m0} = 222 \pm 11\text{ mS/mm}$ . Drain current is highly linear with  $V_{GS}$  over the  $g_m$  plateau, reaching a maximum of  $514 \pm 17\text{ mA/mm}$ , the velocity saturation current limit of the extrinsic channel [3]. This linearity is highly desirable for power applications. The breakdown voltage is 19.4 V, defined as the value of  $V_{DS}$  at which  $I_D = 1\text{ mA/mm}$  with  $V_{GS}$  at threshold ( $-2.4\text{ V}$ ). The reverse gate breakdown voltage is  $-17\text{ V}$  at  $I_G = -10\ \mu\text{A}$ .

Fig. 3 presents both  $f_T$  and  $f_{\text{max}}$  versus  $V_{GS}$  for typical  $L_g = 1.7\text{-}\mu\text{m}$  and  $W_g = 200\text{-}\mu\text{m}$  T-gate MIFET's at  $V_{DS} = 5\text{ V}$ . Both curves show distinct and extremely broad and flat plateaus, with peak  $f_T = 8\text{ GHz}$  and peak  $f_{\text{max}} = 21\text{ GHz}$  and with the  $f_T$  plateau exceeding 90% of peak over a

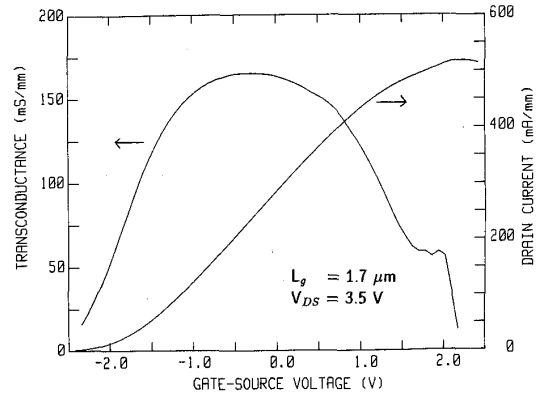


Fig. 2. Statistically averaged  $g_m$  and  $I_D$  versus  $V_{GS}$  for 20 randomly selected  $1.7\text{-}\mu\text{m} \times 30\text{-}\mu\text{m}$  MIFET's ( $V_{DS} = 3.5\text{ V}$ ).

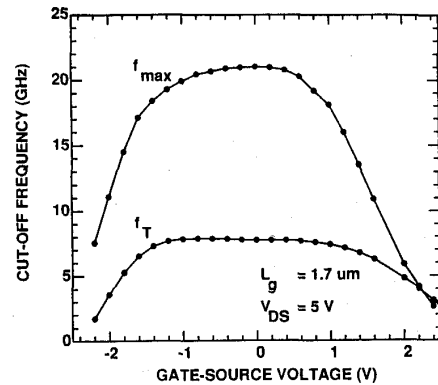


Fig. 3.  $f_T$  and  $f_{\text{max}}$  versus  $V_{GS}$  for a typical  $1.7\text{-}\mu\text{m} \times 200\text{-}\mu\text{m}$  T-gate MIFET ( $V_{DS} = 5\text{ V}$ ).

gate swing of 2.6 V. Because our parasitic  $C_{gs}$  and  $C_{gd}$  are less than 7% of intrinsic  $C_{gs}$ ,  $f_T$  accurately reflects the effective channel electron velocity  $v_e$ , yielding an almost constant  $v_e = 9 \times 10^6\text{ cm/s}$ . Thus, the  $f_T$  and  $f_{\text{max}}$  plateaus provide direct evidence that the pseudomorphic MIFET operates in velocity saturation over most of the useful  $V_{GS}$  swing, as has been observed in InAlAs/InGaAs MIFET's [15], and make the device uniquely suitable for high-frequency large-signal operation.

We also extract the RF transconductance from  $\text{Re}[y_{21}]$ , obtained through the measured  $S$  parameters. Fig. 4 shows  $g_m$  versus  $V_{GS}$  both at dc and 3 GHz. We find almost no difference between the two curves to within the accuracy of the parameter extraction. This lack of frequency dispersion is also evident in capacitance-voltage characterization of  $200\text{-}\mu\text{m} \times 200\text{-}\mu\text{m}$  gate diodes, measured at 10 kHz, 100 kHz, and 1 MHz for  $V_{GS}$  above threshold. Taken together, both  $g_m$  and  $CV$  data encompass an extremely broad-band frequency range, and should reveal dispersion if electrically active traps exist in the AlGaAs pseudoinulator. The lack of any such dispersion indicates high-quality trap-free AlGaAs, and is an important merit of the undoped pseudoinulator MIFET design. In addition, by computing the area beneath  $C_{gs}$  versus  $V_{GS}$  from  $V_{GS} = -1.8\text{ V}$  (threshold voltage in the diode structures) through  $V_{GS} = 0.5\text{ V}$  (beginning of gate

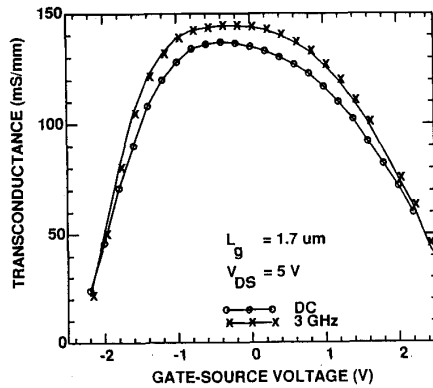


Fig. 4.  $g_m$  versus  $V_{GS}$  for a typical  $1.7\text{-}\mu\text{m} \times 200\text{-}\mu\text{m}$  T-gate MIFET, measured at dc and 3 GHz ( $V_{DS} = 5$  V).

leakage influence), we find a maximum channel electron sheet density of over  $6 \times 10^{12} \text{ cm}^{-2}$ , a value unattainable in a single heterojunction MODFET.

In summary, we demonstrate  $L_g = 1.7\text{-}\mu\text{m}$  pseudomorphic AlGaAs/n<sup>+</sup>-InGaAs/GaAs MIFET's that display a broad  $g_m$  versus  $V_{GS}$  characteristic and thus achieve high drain current linearity and exceptional  $I_{D,\text{max}}$ . We observe extremely broad plateaus in  $f_T$  and  $f_{\text{max}}$  versus  $V_{GS}$ , direct evidence for MIFET operation in velocity saturation over most of the gate swing, and find a lack of frequency dispersion in both  $g_m$  and in  $C_{gs}$  versus  $V_{GS}$  from dc through microwave frequencies. These features combine to make the MIFET well suited to many large-signal, broad-band telecommunications applications.

#### ACKNOWLEDGMENT

The authors gratefully thank B. Meskoob for training on the HP 8510B network analyzer and J. R. Hayes and the staff of Bellcore for discussions and advice.

#### REFERENCES

- [1] H. Hida *et al.*, "A 760 mS/mm N<sup>+</sup> self-aligned enhancement mode doped channel MIS-like FET (DMT)," in *IEDM Tech. Dig.*, 1986, p. 759.
- [2] H. Hida, A. Okamoto, H. Toyoshima, and K. Ohata, "As investigation of i-AlGaAs/n-GaAs doped-channel MIS-like FET's (DMT's)—Properties and performance potentialities," *IEEE Trans. Electron Devices*, vol. ED-34, no. 7, p. 1448, 1987.
- [3] D. R. Greenberg, "The physics of scaling of AlGaAs/n<sup>+</sup>-InGaAs/GaAs heterostructure field-effect transistors," Master's thesis, Mass. Inst. Technol., Cambridge, Sept. 1990.
- [4] K. Hirakawa, H. Sakaki, and J. Yoshino, "Concentration of electrons in selectively doped GaAlAs/GaAs heterojunction and its dependence on spacer-layer thickness and gate electric field," *Appl. Phys. Lett.*, vol. 45, no. 3, p. 253, 1984.
- [5] R. R. Daniels, *et al.*, "Doped channel pseudomorphic GaAs/InGaAs/AlGaAs heterostructure FET's," in *IEDM Tech. Dig.*, 1987, p. 921.
- [6] P. P. Ruden *et al.*, "AlGaAs/InGaAs/GaAs quantum well doped channel heterostructure FET's," *IEEE Trans. Electron Devices*, vol. 37, no. 10, p. 2171, 1990.
- [7] B. Kim *et al.*, "Millimeter-wave power operation of an AlGaAs/InGaAs/GaAs quantum well MISFET," *IEEE Trans. Electron Devices*, vol. 36, no. 10, p. 2236, 1989.
- [8] A. A. Ketterson *et al.*, "Characterization of InGaAs/AlGaAs pseudomorphic modulation-doped field-effect transistors," *IEEE Trans. Electron Devices*, vol. ED-33, no. 5, p. 564, 1986.
- [9] K. Hikosaka, S. Sasa, N. Harada, and S. Kuroda, "Current-gain cutoff frequency comparison of InGaAs HEMT's," *IEEE Electron Device Lett.*, vol. 9, no. 5, p. 241, 1988.
- [10] P. Godts, E. Constant, J. Zimmermann, and D. Depreuw, "Investigation of influence of DX centres on HEMT operation at room temperature," *Electron. Lett.*, vol. 24, no. 15, p. 937, 1988.
- [11] J. Laskar, J. Kolodzey, A. A. Ketterson, I. Adesida, and A. Y. Cho, "Characteristics of GaAs/AlGaAs-doped channel MISFET's at cryogenic temperatures," *IEEE Electron Device Lett.*, vol. 11, no. 7, p. 300, 1990.
- [12] M. Heiblum, E. E. Mendez, and L. Osterling, "Growth by molecular beam epitaxy and characterization of high purity GaAs and AlGaAs," *J. Appl. Phys.*, vol. 54, no. 12, p. 6982, 1983.
- [13] S. Adachi and H. Ito, "Thermal conversion and hydrogenation effects in AlGaAs," *J. Appl. Phys.*, vol. 64, no. 5, p. 2772, 1988.
- [14] E. Kapon, S. Simhony, J. P. Harbison, L. T. Florez, and P. Worland, "Threshold current reduction in patterned quantum well semiconductor lasers grown by molecular beam epitaxy," *Appl. Phys. Lett.*, vol. 56, no. 19, p. 1825, 1990.
- [15] J. A. del Alamo and T. Mizutani, "Bias dependence of  $f_T$  and  $f_{\text{max}}$  in an  $\text{In}_{0.52}\text{Al}_{0.48}\text{As/n}^+\text{-In}_{0.53}\text{Ga}_{0.47}\text{As}$  MISFET," *IEEE Electron Device Lett.*, vol. 9, no. 12, p. 654, 1988.